

Triggering waves in nonlinear lattices: Quest for anharmonic phonons and corresponding mean free paths

Sha Liu,^{1,2,*} Junjie Liu,^{3,1} Peter Hänggi,^{4,5,1,6,†} Changqin Wu,³ and Baowen Li^{1,2,6,7,‡}

¹Department of Physics and Centre for Computational Science and Engineering, National University of Singapore, 117546 Singapore

²NUS Graduate School for Integrative Sciences and Engineering, 117456 Singapore

³State Key Laboratory of Surface Physics and Department of Physics, Fudan University, 200433 Shanghai, China

⁴Institute of Physics, University of Augsburg, Universitätsstr. 1, D-86159 Augsburg, Germany

⁵Nanosystems Initiative Munich, Schellingstr. 4, D-80799 München, Germany

⁶Center for Phononics and Thermal Energy Science, School of Physics Science and Engineering, Tongji University, 200092 Shanghai, China

⁷Graphene Research Centre, Faculty of Science, National University of Singapore, 117542 Singapore

(Dated: 17 Nov 2014)

Guided by a stylized experiment we develop a self-consistent anharmonic phonon concept for nonlinear lattices which allows for explicit “visualization.” The idea uses a small external driving force which excites the front particles in a nonlinear lattice slab and subsequently one monitors the excited wave evolution using molecular dynamics simulations. This allows for a simultaneous, direct determination of the existence of the phonon mean free path with its corresponding anharmonic phonon wavenumber as a function of temperature. The concept for the mean free path is very distinct from known prior approaches: the latter evaluate the mean free path only indirectly, via using both, a scale for the phonon relaxation time and yet another one for the phonon velocity. Notably, the concept here is neither limited to small lattice nonlinearities nor to small frequencies. The scheme is tested for three strongly nonlinear lattices of timely current interest which either exhibit normal or anomalous heat transport.

PACS numbers: 63.20.Ry, 63.20.D-, 66.70.-f, 05.60.Cd

I. INTRODUCTION

In solid phases, phonons are collective, elementary vibrations in harmonic lattices and as such play a prominent role for physical transport phenomena aplenty¹⁻⁴, of which the transport of heat is a most prominent one. In harmonic lattices these phonons constitute nondecaying, stable propagating waves obeying a dispersion relation for angular frequency ω and corresponding wavenumber k . This in turn implies that these phonons possess strictly infinite mean free paths (MFPs). Consequently, heat transport in harmonic lattices is ballistic^{5,6} and thus no temperature gradient can be sustained (breakdown of Fourier’s law).

Generally, however, everyday solid materials are far from being perfect harmonic lattices. Therefore, the phonon concept bears no firm basis *away* from its underlying (effective) harmonic approximation. As pointed out by Peierls long ago^{2,3}, such anharmonicity is essential for Umklapp scattering — an indispensable process for a finite, size-independent thermal conductivity κ in three dimensional (3D) materials. Phenomenologically^{3,4}, the thermal conductivity is approximated in terms of a wave-number-dependent phonon MFP l_k ; i.e. $\kappa = (1/3) \sum_k C_k v_k l_k$. Here, C_k is the specific heat of the phonon mode and v_k its phonon group velocity.

Principally, we encounter the dilemma that the rigorous existence of a phonon excitation in a nonlinear lattice is self-contradictory to the very existence of a finite MFP. Particularly, this concept of a nonlinear or anharmonic phonon may cause considerable unease when dealing with strong nonlinear interaction forces and/or high temperatures where thermal excitations no longer predominantly dwell the harmonic well regions of corresponding interaction potentials. Moreover, the observed breakdown of Fourier’s law with superdiffusive heat

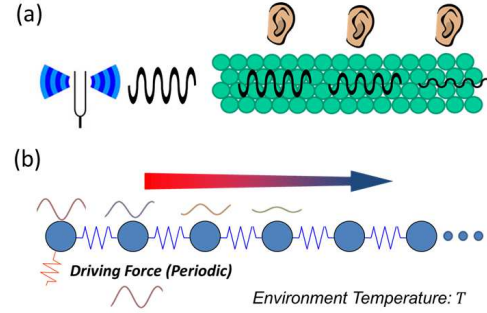


FIG. 1: (color online) Hunting for phonons and MFPs in nonlinear lattices: (a) An illustration of the “tuning fork experiment”; (b) a schematic sketch of the driving force method in a nonlinear lattice.

transport in systems of low dimensions⁷⁻⁹ with a thermal conductivity diverging with increasing length of the sample necessitates that some MFPs must diverge.

One method addressing the issue is the so termed renormalized phonon picture¹⁰⁻¹⁵. In essence, this approach uses an effective harmonic approximation of the nonlinear interaction forces via a temperature-renormalized phonon dispersion. Such renormalized phonon theory, however, neither determines the phonon MFP nor a phonon relaxation time (or, likewise, a phonon lifetime). The problem of finite MFPs and corresponding relaxation times thus remains open. One possibility addressing the missing link consists in combining approximate Boltzmann transport theory for heat transport with a single mode relaxation time approximation^{16,17}. In fact, while this phenomenological scheme is commonly adopted nowadays, its regime of validity has never been justified from first principles^{18,19}.

In summary, the present state of the art is that the physical value for this thermal MFP ℓ is evaluated *indirectly* only: Its evaluation involves both a characteristic relaxation time or lifetime scale τ and as well a characteristic scale for the phonon speed v , yielding $\ell = v\tau$. Thus, this MFP is not uniquely given in the sense that various time scales come to mind; namely, the so termed phonon lifetime (as obtained from Lorentzian fit) in prior phonon quasiparticle studies in the reciprocal lattice space^{20–28}, a phonon collision time or transport relaxation time (notably being not equivalent with the phonon lifetime) as obtained from a Peierls–Boltzmann approach are just but a few^{29,30}. Likewise, the *a priori* choice for the speed scale taken as the group velocity is also empirical. – Consequently, a direct, molecular dynamics (MD) based visualization rendering this much sought-after, physically descriptive and useful phonon MFP is highly desirable.

Here, we put forward an experiment-inspired theoretical scheme for propagating anharmonic phonons (a-phs) when ubiquitous nonlinear interaction forces are ruling the lattice dynamics. Our main objective is to significantly advance an a-ph concept that simultaneously solves the following challenges: (i) the concept can be evaluated by MD simulations and additionally allows for the visualization of the physical existence of the a-ph’s together with their MFPs, (ii) the concept is manifest nonperturbative in the strength of lattice nonlinearities, and additionally, (iii) the concept is neither restricted to low temperature nor to low frequencies.

II. TRIGGERING ANHARMONIC PHONONS.

To elucidate whether a phonon picture still holds in strongly nonlinear solids we use a “tuning fork experiment” as sketched with Fig. 1(a). Here, a tuning fork operating at small driving strength and at a fixed frequency ω is placed in front of a crystalline, nonlinear lattice slab held at a temperature T . This driving source will generate sound that propagates along the slab. For a phonon picture to hold up, it is then required that the propagating disturbance physically causes a collective, attenuated plane wave-like response. For the MFP to exist, the spatially dependent wave amplitude preferably is required to exhibit an exponential decay with a single scale vs increasing spatial spread. If so, this renders the sought-after MFP for a-ph’s in a nonlinear lattice. The a-ph may still hold up, however, even if the attenuation of the propagating wave occurs non-exponentially, i.e., when exhibiting multiple spatial scales, see below.

The driving source triggering the thermal phonons must be set sufficiently small so that no nonlinear, non-phonon-like excitations become excited. This implies that the triggered response of the tuning fork occurs solely within its linear regime, i.e., the output signal occurs at the same (driving) frequency only³¹.

To realize this stylized experiment, we start with the lattice being held at thermal equilibrium. We next apply an time-dependent external weak force $f_d(t) = f_1 \cos \omega t$, see in Fig. 1(b), to the first particle and measure the resulting long time response occurring at all the remaining particles. For the

a-ph concept to make sense this collective response must assume the form of a propagating plane wave, i.e., the thermally averaged velocity $v_n(t)$ of the n -th particle is required to read for $n = 1, 2, \dots$:

$$\langle v_n(t) \rangle_f = |A_n| \cos(\omega t + \phi_n) = \text{Re}(|A_n| e^{i(\phi_n + \omega t)}), \quad (1)$$

with the phase obeying

$$\phi_n = -kn + \phi_0. \quad (2)$$

In the expression, $\langle \cdot \rangle_f$ denotes the statistical average under the influence of the driving force. This so parameterized excited motion defines an effective phonon with a frequency ω that precisely matches the input driving frequency ω . The coefficient, $k = -d\phi_n/dn$, plays the role of the wavenumber k . With the amplitude $|A_n|$ assumed to decay exponentially as

$$|A_n| \propto e^{-n/\ell}, \quad (3)$$

its decay length ℓ provides the searched MFP for this a-ph.

For the sake of simplicity, we first formulate the concept for one-dimensional (1D) lattices. The scheme can readily be generalized to higher dimensions and complex materials by applying forces to atoms lying on a chosen lattice plane that trigger either longitudinal or transverse waves which propagate perpendicular to the plane, which will be discussed in Sec. II B.

The 1D lattice Hamiltonian assumes the general dimensionless form³²:

$$H_0 = \sum_{n=1}^N \left[\frac{p_n^2}{2} + V(x_{n+1} - x_n) + U(x_n) \right], \quad (4)$$

where p_n and x_n denote the momentum and displacement from the equilibrium position for the n -th particle (with unit mass), respectively, $V(x_{n+1} - x_n)$ is the inter-particle potential and $U(x_n)$ denotes a possibly present on-site potential. Following the common approach we employ the periodic boundary conditions. The role of finite temperature T enters by using a canonical ensemble with the unperturbed distribution reading, $\rho_{eq} = Z^{-1} \exp[-\beta_T H_0]$, where $\beta_T = 1/k_B T$ is the inverse temperature and Z the canonical partition function.

Following the spirit of the “tuning fork experiment”, we then apply a weak single-frequency signal $f_d(t)$ to the first particle of the lattice. Therefore, the total Hamiltonian of the system reads

$$H_{tot} = H_0 + H_{ext} = H_0 - f_d(t)x_1. \quad (5)$$

We can then calculate the thermally averaged velocity at each site n using canonical linear response theory^{31,34}, yielding:

$$\begin{aligned} \langle v_n(t) \rangle_f &= \beta_T \int_{-\infty}^t ds \langle v_n(t-s)v_1(0) \rangle f_d(s), \\ &= \beta_T \int_0^{\infty} d\tau \langle v_n(\tau)v_1(0) \rangle f_d(t-\tau) \end{aligned} \quad (6)$$

where $\langle \cdot \rangle$ denotes the canonical ensemble average.

For $f_d(t) = f_1 \cos \omega t$, the excited motion can equivalently be cast into the form of Eq. (1), which involves the Fourier transformed susceptibility, i.e.,

$$\langle v_n(t) \rangle_f = f_1 \text{Re}[\chi_n(\omega) e^{i\omega t}], \quad (7)$$

where the susceptibility $\chi(\omega)$ reads

$$\chi_n(\omega) = \beta_T \int_0^\infty d\tau \langle v_n(\tau) v_1(0) \rangle e^{-i\omega\tau} \equiv |\chi_n| e^{i\phi_n}. \quad (8)$$

This appealing result allows one to assign the existence of an a-ph and its corresponding MFP: (i) an a-ph exists with a wavenumber $k(\omega)$ if and only if the linear relationship in (2) is fulfilled and (ii) possesses a unique MFP $\ell(\omega)$ when $|\chi_n(\omega)| \propto \exp[-n/\ell(\omega)]$. Importantly, the phonon response amplitude $|\chi_n(\omega)|$ and its phase $\phi_n(\omega)$ now both attain a dependence on temperature T . The wavevector is given by $k(\omega, T) = -d\phi_n(\omega, T)/dn$. This very form considerably simplifies the numerical efforts as compared to directly studying the excited waves via the MD method, i.e., one finds the whole frequency-resolved phonon properties at once.

As an expectation, this so introduced a-ph concept should be naturally consistent with the normal phonon in harmonic lattices. Such a fact can be readily tested analytically without invoking the linear response theory, which we demonstrate below. Following this, we give a brief extension of our method to the more general three dimensional case and then move on to the application of our method.

A. Harmonic Lattices

For a harmonic lattice with potentials $V(x) = \frac{1}{2}x^2$ and $U(x) = 0$, we expect to observe from our method that the MFPs are infinite with the wavenumber k satisfying

$$k(\omega) = 2 \arcsin \frac{\omega}{2}. \quad (9)$$

To see this, we apply periodic boundary conditions to the lattice so that $x_{0/1} = x_{N/N+1}$ and $p_{0/1} = p_{N/N+1}$. With a periodic driving force $f_d = f_1 \cos \omega t$ switched in the infinite past and applied to the first particle in a 1D-chain, the equations of motion (EOMs) can be put into a compact matrix form, reading

$$\ddot{\mathbf{x}} = -\mathbf{\Phi} \mathbf{x} + \mathbf{F}(t). \quad (10)$$

Here, $\mathbf{\Phi}$ is the force matrix with elements $\Phi_{i,j} = 2\delta_{i,j} - \delta_{i,j-1} - \delta_{i,j+1}$ in terms of the Kronecker delta function $\delta_{i,j}$, and $\mathbf{F} = \mathbf{f} \cos(\omega t) = (f_1, 0, \dots, 0)^T \cos(\omega t)$. Its solution is additive due to $\mathbf{F}(t)$ entering a linear equation of motion. Thus, the excitations of $\mathbf{F}(t)$ can be obtained by Fourier transformation, reading

$$\langle \mathbf{x}(t) \rangle_f = \int_{-\infty}^{\infty} \mathbf{G}(\omega') \tilde{\mathbf{F}}(\omega') e^{i\omega' t} d\omega', \quad (11)$$

where $\tilde{\cdot}$ denotes a Fourier transform and \mathbf{G} is the phonon Green's function

$$\mathbf{G}(\omega') = (\mathbf{\Phi} - \omega'^2)^{-1}. \quad (12)$$

For a driving $f_d = f_1 \cos \omega t$, it can then be calculated that the resulting excited motion reads

$$\langle x_n(t) \rangle_f = f_1 \text{Re} [\mathbf{G}_{n,1}(\omega) e^{i\omega t}], \quad (13)$$

and consequently

$$\langle v_n(t) \rangle_f = f_1 \text{Re} [i\omega \mathbf{G}_{n,1}(\omega) e^{i\omega t}], \quad (14)$$

which has the same form as (7) with $\chi_n(\omega) = i\omega \mathbf{G}_{n,1}$.

Due to the cyclic structure of the matrix $\mathbf{\Phi} - \omega^2$, its inverse \mathbf{G} can be analytically obtained. Its first column reads

$$\mathbf{G}_{n,1} = -\frac{\cos(\frac{N}{2} - n + 1)z}{2 \sin(Nz/2) \sin z}, \quad (15)$$

The second column is obtained by cyclically shifting the first column by one element. The third column is obtained by cyclically shifting the first column by two elements, and so on. In the formula, $e^{\pm iz}$ are the two roots of the quadratic equation $-1 + (2 - \omega^2)x - x^2 = 0$. Therefore, z satisfies

$$\cos z = 1 - \frac{\omega^2}{2}, \quad (16)$$

which can be verified by substitution.

For $0 < \omega < 2$, z is a real number. According to (14) and (15), the velocity of excited wave varies with n as

$$\langle v_n(t) \rangle_f \sim \cos \left[\left(\frac{N}{2} - n + 1 \right) z \right] \sin \omega t. \quad (17)$$

It represents a standing wave formed by two plane waves with the same wavenumber $k = z$ satisfying

$$\omega = 2 \sin \frac{k}{2}, \quad (18)$$

which just yields the intrinsic dispersion relation for the harmonic lattice. The plane wave nature also implies the excited waves have infinite MFPs.

Note that the derivation above is exact and beyond a linear response. However, it can be shown that applying (7) and (8) to the harmonic lattice will give exactly the same result in (14) and (15), due to the fact that for harmonic lattices all higher order response terms are actually zero and only the linear response term is present.

B. Generalization to higher dimensions

In order to generalize our method to higher dimensional cases, we must apply a periodic driving force at the same frequency to each particles in a plane. Taking the three dimensional (3D) case as example, if we want to study the wave propagation along the direction $\mathbf{k} = h\mathbf{b}_1 + k\mathbf{b}_2 + l\mathbf{b}_3$ where

\mathbf{b}_1 , \mathbf{b}_2 , and \mathbf{b}_3 are the primitive vectors in the reciprocal lattice, we first choose a plane with Miller indices (hkl) , denoted as α , being orthogonal to the direction \mathbf{k} . Then, we apply forces to all particles in this plane. To trigger longitudinal waves, we apply out-of-plane forces that are perpendicular to the plane. To trigger transverse waves, we apply in-plane forces.

With such an setup, (6) can be easily generalized to read

$$\langle v_n^d(t) \rangle_f = \beta_T \sum_{i \in \alpha} \int_0^\infty d\tau \langle v_n^d(\tau) v_i^d(0) \rangle f_i^d(t - \tau), \quad (19)$$

where $i \in \alpha$ means particle i is in plane α and $d = \perp$ or \parallel which specifies whether the direction of the force and velocity is out-of-plane (\perp) or in-plane (\parallel). We now identically set $f_i^d(t) = f_\alpha^d(t)/N_\alpha$ (N_α is the number of particles in that plane) for all $i \in \alpha$; then (19) can be simplified to read

$$\langle v_n^d(t) \rangle_f = \beta_T \int_0^\infty d\tau \langle v_n^d(\tau) v_\alpha^d(0) \rangle f_\alpha^d(t - \tau), \quad (20)$$

where $v_\alpha^d = (1/N_\alpha) \sum_{i \in \alpha} v_i^d$ denotes the average velocity for all particles in the plane α .

We can further take an average for all particles in the same lattice plane, denoted as β , which has the same Miller index (so that it is parallel to α) but contains the n -th particle. Therefore, we obtain for the average velocity for that very plane the result

$$\langle v_\beta^d(t) \rangle_f = \beta_T \int_0^\infty d\tau \langle v_\beta^d(\tau) v_\alpha^d(0) \rangle f_\alpha^d(t - \tau). \quad (21)$$

From this result we can infer whether an anharmonic phonon with a wavevector pointed towards the same direction of \mathbf{k} exists or not, by following the same reasoning used for one dimensional lattices.

Note that the derivation is independent of the form of the Hamiltonian H_0 . So the method is equally applicable to study wave transport in inhomogeneous lattices, such as junctions formed by different materials.

III. NUMERICAL DETAILS

We will apply our concept to three archetype 1D nonlinear lattices of varying complexity. Before we move on to study these models in detail, we first describe the numerical details used to detect the anharmonic phonons.

We use throughout a fourth order symplectic $cSABA_2$ algorithm to integrate the Hamiltonian equations of motion³⁵. The time step has always been chosen as $h = 0.02$ and the length has been set at $N = 2048$, using periodic boundary conditions, for all models studied. At the beginning of each simulation, a total time $t = 2 \times 10^6$ is used to thermally equilibrate the system. After that, the time-homogeneous equilibrium velocity correlation $\langle v_n(t) v_1(0) \rangle$ is calculated by using the time average which replaces, using ergodicity for the nonlinear lattice, the corresponding ensemble average. An average over 3.2×10^9 steps is used. The correlation $\langle v_n(t) v_1(0) \rangle$ is calculated for each $n = 1, 2, \dots, N$ and $t = 0, h, 2h, \dots, t_{\max}$.

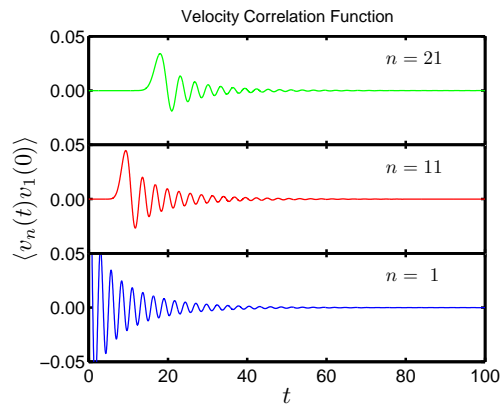


FIG. 2: (Color online) The velocity auto-correlation $\langle v_n(t) v_1(0) \rangle$ of the FPU- β model for $n = 1, 11, 21$. The simulation is carried out on an FPU- β lattice with length $N=2048$ at temperature $T = 0.2$.

Afterwards, $\chi_n(\omega)$ is obtained by taking a Fourier transform according to Eq. (7).

The upper time limit t_{\max} is properly chosen such that the excited waves along the periodic ring of size N do not overlap with each other for $t \in (0, t_{\max})$. Namely, $t_{\max} < N/2v_s$ where v_s is the largest group velocity of the phonons studied, i.e., the corresponding sound velocity. On the other hand, this t_{\max} determines the frequency resolution. The larger t_{\max} is, the smaller is the frequency resolution. Specifically, $t_{\max} = 655.36$ has been used for all three models.

A few samples of the velocity correlation $\langle v_n(t) v_1(0) \rangle$ are depicted in Fig. 2 for the Fermi-Pasta-Ulam (FPU)- β lattice at a temperature $T = 0.2$. $\chi_n(\omega)$ is then calculated via the Fourier transformation according to Eq. (7). For the other models, we also observe similar oscillation behavior for the velocity-velocity correlation function.

IV. DETECTING ANHARMONIC PHONONS.

In this section, we apply our method to study three archetype 1D nonlinear lattices. Of timely interest in the context of anomalous vs. normal heat conduction are the FPU- β lattice, the FPU- $\alpha\beta$ lattice and the ϕ^4 lattice. Our numerical simulations shall cover extended regimes of temperature T and frequencies ω .

A. FPU- β lattice.

The prevalently studied nonlinear 1D lattice dynamics in the literature is the FPU- β dynamics with $V(x) = \frac{1}{2}x^2 + \frac{1}{4}x^4$ and $U(x) = 0$ ^{36,37}. Its lattice dynamics has been demonstrated to exhibit superdiffusive heat transport^{7-9,38}.

Applying the a-ph concept, our findings are depicted in Fig. 3 for $\chi_n(\omega)$ vs. lattice sites n , for different driving frequencies $\omega \in (0.0096, 2.675)$ and a dimensionless temperature $T = 0.2$ ³². Beyond $\omega = 2.675$ the response decays very

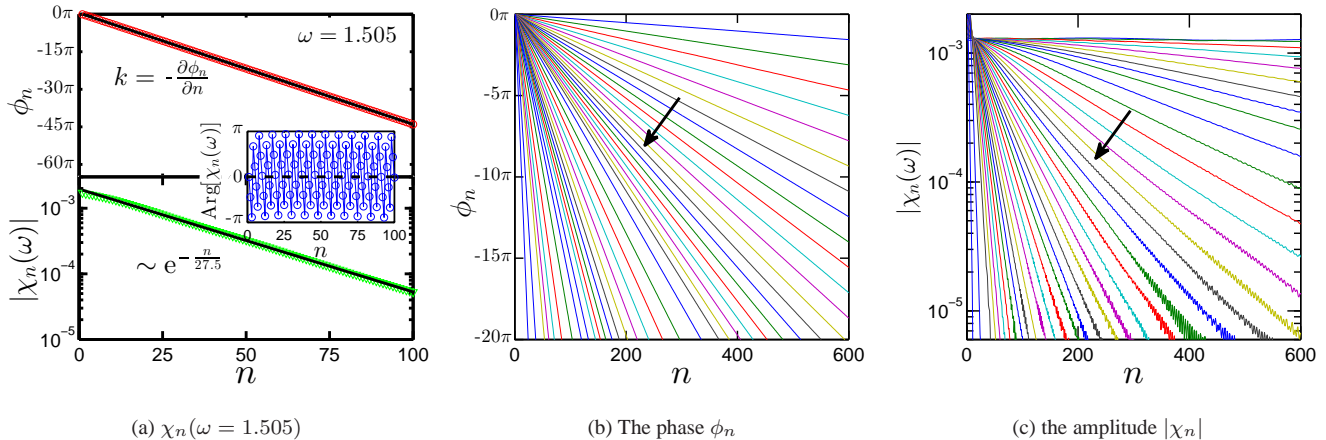


FIG. 3: (Color online) The response function for an FPU- β chain with length $N = 2048$ at temperature $T = 0.2$. (a) A detailed example for $\chi_n(\omega)$ at frequency $\omega = 1.505$ as a function of n . The upper panel shows the phase ϕ_n and the lower panel shows the amplitude $|\chi_n|$. The inset shows the principal values of the arguments $\text{Arg}[\chi_n] \in [-\pi, \pi)$. The principal value jumps discontinuously by 2π when $-\pi$ is reached. To obtain a continuous varying phase ϕ_n , as depicted in the upper panel, we shift the arguments by 2π after each such jump. (b), (c): A comprehensive view of the phase and the amplitude, respectively, for different frequencies $\omega \in (0.0096, 2.675)$. The driving frequency ω increases along the arrow.

fast, yielding also a very short phonon MFP. This limits the evaluation of the corresponding wavenumber k —practically, it cannot be extracted with good confidence near $k \approx \pi$.

The results in Fig. 3 provide twofold relevant information:

(i) Firstly, for all frequencies depicted, the phase ϕ_n perfectly decreases linearly with n . This corroborates the existence of a-ph's with a corresponding wavenumber $k = -d\phi_n/dn$. We evaluate $k(\omega)$ for different driving frequencies ω , as depicted in Fig. 4(a), and compare our results with predictions taken from renormalized phonon theory (dashed lines)^{14,15}, which predicts

$$\omega = 2\alpha(T) \sin \frac{k}{2}. \quad (22)$$

Here, $\alpha(T)$ denotes the temperature-dependent renormalization factor that quantifies the strength of nonlinearity. The temperature dependent sound speed v_s emerges as $v_s = \frac{d\omega}{dk}|_{k=0} = \alpha(T)$. For the FPU- β lattice $\alpha(T) =$

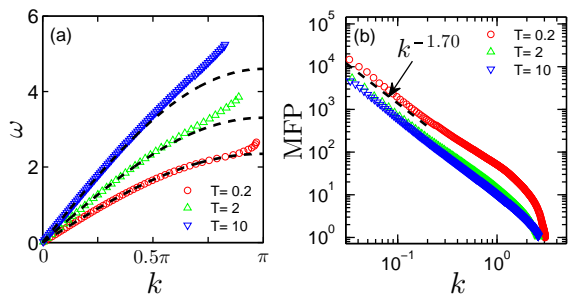


FIG. 4: (Color online) (a) The dispersion relation for the FPU- β model. The dashed curve are obtained from the renormalized phonon theory using Eq. (22). (b) Corresponding phonon MFPs. The dashed lines are illustrations for a power-law behavior $\ell \sim k^{-1.70}$.

$(1 + \frac{\int x^4 e^{-(x^2/2+x^4/4)/T} dx}{\int x^2 e^{-(x^2/2+x^4/4)/T} dx})^{1/2}$ ^{14,15}; it increases with temperature, starting out at 1. As seen in Fig. 4(a), excellent agreement is obtained for low frequency a-ph's. The differences between the a-ph concept and renormalized phonon theory occur at large frequencies, with deviations slightly increasing with increasing temperature. This corroborates with the fact that effective phonon theory self-consistently applies to weak anharmonic forces and long wavelength phonons only.

(ii) Secondly, within the depicted frequency regime the amplitude $|\chi_n|$, Fig. 3(c), perfectly decays exponentially with increasing n . Therefore, a sensible MFP ℓ is obtained for each a-ph, cf. in Fig. 4(b), where we depict the MFPs at three different ambient temperatures. Moreover, the MFPs diverge with the decreasing wavenumber k . This is a salient feature known for momentum conserving 1D systems³⁹.

Interestingly, a power-law divergence $\ell(k) \sim k^{-\mu}$ with $\mu \approx 1.70$ is observed for small k for various temperatures. The numerical result closely matches the prediction of Peierls-Boltzmann theory at weak anharmonic nonlinearity, rendering $\mu = 5/3$ ^{19,40,41}. A divergent exponent $\mu > 1$ causes an anomalous divergent heat conductivity $\kappa \sim N^\beta$ with $\beta = 1 - 1/\mu$ ^{8,19}. Therefore, we numerically find $\beta \approx 0.411$, which is close to results in^{38,42}.

We stress that with our concept of the a-ph the existence of MFPs (or its corresponding transport relaxation time τ_k) in the FPU- β lattice is here not postulated *a priori*^{19,40,41} but is confirmed independently via MD simulations in configuration space.

B. FPU- $\alpha\beta$ lattice.

The FPU- $\alpha\beta$ lattices containing a non-vanishing cubic term $V(x) = \frac{1}{2}x^2 + \frac{1}{3}x^3 + \frac{1}{4}x^4$ and $U(x) = 0$ distinctly differ from

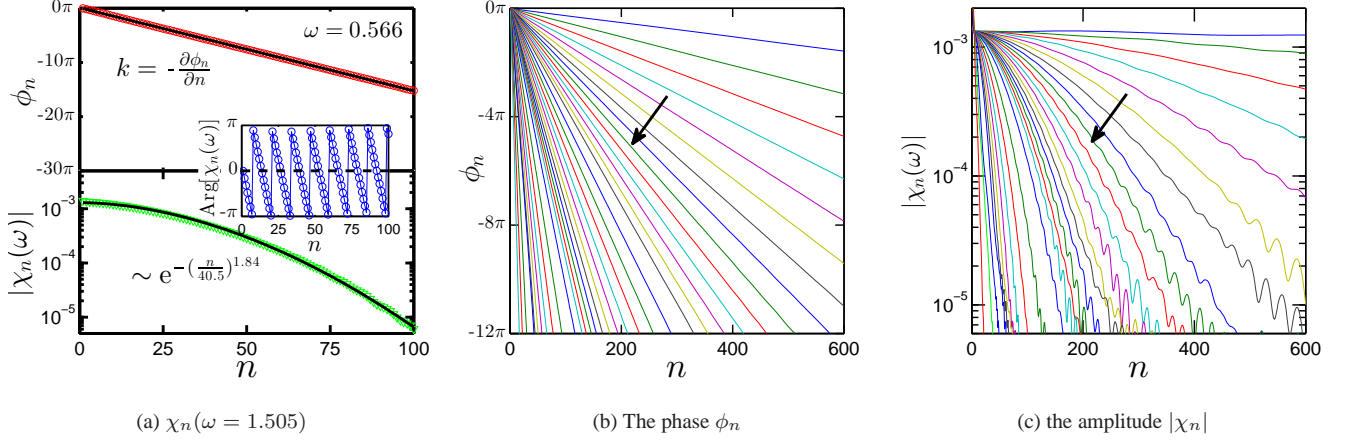


FIG. 5: (color online) The response function for an FPU- $\alpha\beta$ chain with length $N = 2048$ at temperature $T = 0.2$. (a) A detailed example for $\chi_n(\omega)$ at frequency $\omega = 0.566$. The upper panel shows the phase ϕ_n and the lower panel shows the amplitude $|\chi_n|$. The inset shows the principal values of the arguments $\text{Arg}[\chi_n] \in [-\pi, \pi]$. The principal value jumps discontinuously by 2π when $-\pi$ is reached. To obtain a continuous varying phase ϕ_n , as depicted in the upper panel, we shift the arguments by 2π after each such jump. (b), (c) A comprehensive view of the phase and the amplitude for different frequencies, respectively, $\omega \in (0.0096, 2.387)$. The driving frequency ω increases along the arrow.

FPU- β lattices. The inherent asymmetry of the interaction potential yields a nonvanishing internal pressure^{43,44}. Figure 5 depicts the response function for the FPU- $\alpha\beta$ lattice.

As shown in Fig. 5(b), the perfect linear dependence of the phases ϕ_n on n can still be observed. Therefore, it corroborates the existence of a-ph's in the FPU- $\alpha\beta$ case.

The amplitudes $|\chi_n|$, as shown in Fig. 5(c), however, deviate from an exponential decay but instead depict multiple scales. Therefore, a strict MFP cannot be defined. Interestingly, as depicted as an example in Fig. 5(a), their behavior can be fitted with a stretched exponential

$$|\chi_n(\omega)| = |\chi_1(\omega)| \exp\left(-\frac{(n-1)^a}{l^a}\right) \quad (23)$$

with a frequency dependent parameter a . Therefore, an effective single scale ℓ_{eff} can still be defined for each frequency ω

if we average over all scales, i.e.,

$$\ell_{\text{eff}}(\omega) := \sum_1^\infty \frac{|\chi_n(\omega)|}{|\chi_1(\omega)|} \approx \int_0^\infty \exp\left(-\frac{n^a}{l^a}\right) dn \approx \frac{l}{a} \Gamma\left(\frac{1}{a}\right), \quad (24)$$

where $\Gamma(x)$ is the Gamma function. The dispersion relation and the so obtained effective MFPs are displayed in Fig. 6.

Although a renormalized phonon theory for FPU- $\alpha\beta$ lattices does not exist, we still find that Eq. (22) holds approximately true for the dispersion of our a-ph's, see the dashed lines in Fig. 6. The corresponding sound speed $\alpha(T)$ matches well a recent result in⁴⁵, which reads

$$\alpha^2 = \frac{\frac{1}{2}\beta_T^{-2} + \langle V + px; V + px \rangle}{\beta_T (\langle x; x \rangle \langle V; V \rangle - \langle x; V \rangle^2) + \frac{1}{2}\beta_T^{-1} \langle x; x \rangle}, \quad (25)$$

where $V(x)$ is the potential, $\langle A; B \rangle$ denotes the covariance $\langle AB \rangle - \langle A \rangle \langle B \rangle$ for any two quantities A and B , and p is the internal pressure.

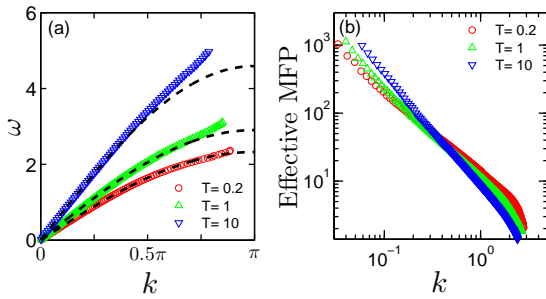


FIG. 6: (color online) (a) The dispersion relation for the FPU- $\alpha\beta$ model at different temperatures. The dashed curves are obtained from (22) with $\alpha(T)$ set at the sound speed as theoretically derived in Ref.⁴⁵. (b) The effective MFPs.

C. ϕ^4 -lattice.

Here, the inter-particle potential is $V(x) = \frac{1}{2}x^2$ together with an on-site potential $U(x) = \frac{1}{4}x^4$. For this momentum-nonconserving nonlinear lattice we still find that the phase follows a perfect linear decay. Moreover, the corresponding MFP for the a-ph exists with a single scale, i.e., $|\chi_n(\omega)|$ nicely decays exponentially (figures for $\chi_n(\omega)$ are similar to Fig. (3) so they are not shown here).

Our proposed a-ph concept holds up also in the presence of an onsite interaction. The dispersion relation and the related MFPs are depicted in Fig. 7. Consistent with the validity of Fourier's law for momentum non-conserving systems the

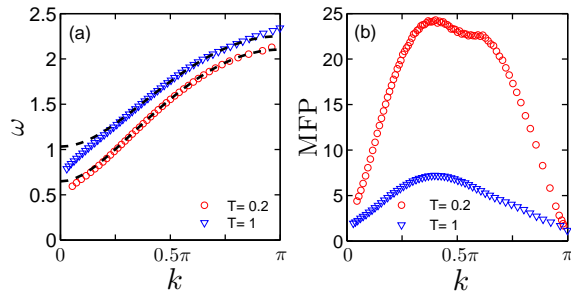


FIG. 7: (color online) (a) Phonon dispersion relation for a ϕ^4 nonlinear lattice at different temperatures. The dashed curves are obtained from renormalized phonon theory⁴⁸. (b) Corresponding anharmonic phonon MFP-behavior.

long wavelength phonons exhibit finite MFPs^{46,47}. Our result for the dispersion relation agrees well with the renormalized phonon theory⁴⁸, namely,

$$\omega = \sqrt{4 \sin^2 \frac{k}{2} + \sigma}; \quad \sigma = \frac{\sum_{i=1}^N \langle x_i^4 \rangle}{\sum_{i=1}^N \langle x_i^2 \rangle}. \quad (26)$$

V. SUMMARY AND DISCUSSION.

The challenge of identifying phonon excitations in strongly nonlinear lattices beyond their corresponding harmonic approximation, termed here anharmonic phonons (a-ph's), has been tackled with MD via a theoretically imposed “tuning fork experiment”. Doing so enables one to account for the role of temperature, large frequencies and lattice nonlinearity in the strong nonlinearity regime. This experiment-inspired phonon concept has been successfully tested over extended parameter regimes of frequency and temperature for three archetype

1D nonlinear lattice models. Note that a temperature dependent phonon MFP is typically not accessible with prior theories without making reference to additional assumptions^{16–19}. Physically, the MFP relates to a phonon transport relaxation time which generally does *not* equal the phonon lifetime³⁰.

Our concept for the MFP holds up beyond the validity regime of renormalized phonon theories^{10–15}, depicting a single, exponentially decaying scale for both the FPU- β lattice, exhibiting anomalous heat conduction, and the ϕ^4 lattice, exhibiting a Fourier’s law behavior. The case of the FPU- $\alpha\beta$ lattice turned out intriguing in that the MFPs no longer exhibit a single scale but decay with multiple scales.

A hallmark of our scheme is that the existence of the a-ph’s and their MFPs is not postulated *a priori*, but instead is physically corroborated by following the propagation of traveling waves with an experiment. The outcome then either validates, or possibly also invalidates, the existence of a-ph with a finite MFP. Our scheme thus distinctly differs from existing phonon quasiparticle concepts^{20–24,26,27}. A most characteristic feature within our scheme is that here we *directly* search for the existence of an a-ph MFP.

The presented a-ph concept allows one to characterize as well infinite MFPs and multiple spatial decay scales, all being features that crucially impact anomalous thermal transport in low-dimensional systems. This a-ph concept may as well spur interest in describing heat transport in 3D materials, encompassing engineered complex materials, such as phononic metamaterials^{49–51}.

Acknowledgments

This work is supported by R-144-000-305-112 from MOE T2 (Singapore). The authors would like to thank Dr. N. Li and Dr. J. Ren for useful discussions.

* Electronic address: phyliaus@nus.edu.sg

† Electronic address: hanggi@physik.uni-augsburg.de

‡ Electronic address: phylibw@nus.edu.sg

¹ M. Born and K. Huang, *Dynamical Theory of Crystal Lattices* (Oxford University Press, Oxford, 1954).

² R. E. Peierls, *Ann. Phys. (N.Y.)* **3**, 1055 (1929).

³ R. E. Peierls, *Quantum Theory of Solids* (Oxford University Press, London, 1955).

⁴ J. M. Ziman, *Principles of the theory of solids*, 2nd ed. (Cambridge University Press, Cambridge, 1972).

⁵ Z. Rieder, J. L. Lebowitz, and E. Lieb, *J. Math. Phys.* **8**, 1073 (1967).

⁶ D. Segal, A. Nitzan and P. Hänggi, *J. Chem. Phys.* **119**, 6840 (2003).

⁷ S. Lepri, R. Livi, and A. Politi, *Phys. Rep.* **377**, 1 (2003).

⁸ A. Dhar, *Adv. Phys.* **57**, 457 (2008).

⁹ S. Liu, X. Xu, R. Xie, G. Zhang and B. Li, *Eur. Phys. J. B* **85**, 337 (2012).

¹⁰ C. Alabiso, M. Casartelli, and P. Marenzoni, *J. Stat. Phys.* **79**, 451 (1995).

¹¹ C. Alabiso and M. Casartelli, *J. Phys. A* **34**, 1223 (2001).

¹² B. Gershgorin, Y. V. Lvov, and D. Cai, *Phys. Rev. Lett.* **95**, 264302 (2005).

¹³ B. Gershgorin, Y. V. Lvov, and D. Cai, *Phys. Rev. E* **75**, 046603 (2007).

¹⁴ N. Li, P. Tong, and B. Li, *Europhys. Lett.* **75**, 49 (2006).

¹⁵ N. Li, B. Li, and S. Flach, *Phys. Rev. Lett.* **105**, 054102 (2010).

¹⁶ J. Callaway, *Phys. Rev.* **113**, 1046 (1959).

¹⁷ M. Holland, *Phys. Rev.* **132**, 2461 (1963).

¹⁸ C. Herring, *Phys. Rev.* **95**, 954 (1954).

¹⁹ A. Pereverzev, *Phys. Rev. E* **68**, 056124 (2003).

²⁰ A. Henry and G. Chen, *J. Comput. Theor. Nanosci.* **5**, 141 (2008).

²¹ J. E. Turney, E. S. Landry, A. J. H. McGaughey and C. H. Amon, *Phys. Rev. B* **79**, 064301 (2009).

²² J. A. Thomas, J. E. Turney, R. M. Iutzi, C. H. Amon and A. J. H. McGaughey, *Phys. Rev. B* **81**, 081411(R) (2010).

²³ T. Sun, X. Shen and P. B. Allen, *Phys. Rev. B* **82**, 224304 (2010).

²⁴ D.-B. Zhang, T. Sun and R. M. Wentzcovitch, *Phys. Rev. Lett.* **112**, 058501 (2014).

²⁵ A. Maradudin and A. Fein, *Phys. Rev.* **128**, 2589 (1962).

- ²⁶ W. M. Collins and H. R. Glyde, Phys. Rev. B **18**, 1132 (1978).
- ²⁷ P. M. Chaikin and T. C. Lubensky, *Principles of Condensed Matter Physics*, (Cambridge University Press, Cambridge, 2000), see Sect. 7.7.
- ²⁸ J. W. L. Pang, W. J. L. Buyers, A. Chernatynskiy, M. D. Lumsden, B. C. Larson and S. R. Phillpot, Phys. Rev. Lett. **110**, 157401 (2013).
- ²⁹ A. Ward and D. A. Broido, Phys. Rev. B **81**, 085205 (2010).
- ³⁰ T. Sun and P. B. Allen, Phys. Rev. B **82**, 224305 (2010).
- ³¹ P. Hänggi and H. Thomas, Phys. Rep. **88**, 207 (1982).
- ³² Following the Appendix in Ref.³³, we choose the atom mass m , the lattice constant a , the force constant k_0 and the Boltzmann constant k_B as the four basic units to scale all physical quantities involved to dimensionless quantities.
- ³³ N. Li, J. Ren, L. Wang, G. Zhang, P. Hänggi, and B. Li, Rev. Mod. Phys. **84**, 1045 (2012).
- ³⁴ R. Kubo, M. Toda, and N. Hashitsume, *Statistical Physics II* (Springer, Berlin, 1991).
- ³⁵ J. Laskar and P. Robutel, Celest. Mech. Dyn. Astron. **80**, 39 (2001).
- ³⁶ J. Ford, Phys. Rep. **213**, 271 (1992).
- ³⁷ G. P. Berman and F. M. Izrailev, Chaos **15**, 015104 (2005).
- ³⁸ S. Lepri, R. Livi, and A. Politi, Phys. Rev. Lett. **78**, 1896 (1997).
- ³⁹ S. Lepri, R. Livi, and A. Politi, Europhys. Lett. **43**, 271 (1998).
- ⁴⁰ B. Nickel, J. Phys. A: Math. and Theor. **40**, 1219 (2007).
- ⁴¹ J. Lukkarinen and H. Spohn, Comm. Pure Appl. Math. **61**, 1753 (2008).
- ⁴² L. Wang and T. Wang, Europhys. Lett. **93**, 54002 (2011).
- ⁴³ Y. Zhong, Y. Zhang, J. Wang, and H. Zhao, Phys. Rev. E **85**, 060102 (2012).
- ⁴⁴ L. Wang, B. Hu, and B. Li, Phys. Rev. E **88**, 052112 (2013).
- ⁴⁵ H. Spohn, J. Stat. Phys. **154**, 1191 (2014): see Eq. (8.32) therein.
- ⁴⁶ B. Hu, B. Li, and H. Zhao, Phys. Rev. E **61**, 3828 (2000).
- ⁴⁷ K. Aoki and D. Kusnezov, Phys. Lett. A **265**, 250 (2000).
- ⁴⁸ N. Li and B. Li, Phys. Rev. E **87**, 042125 (2013).
- ⁴⁹ J. K. Yu, S. Mitrovic, D. Tham, J. Varghese, and J. R. Heath, Nat. Nanotechnol. **5**, 718 (2010).
- ⁵⁰ L. Yang, N. Yang and B. Li, Nano Lett., **14**, 1734 (2014).
- ⁵¹ B. L. Davis and M. I. Hussein, Phys. Rev. Lett. **112**, 055505 (2014).

